J. Fluid Mech. (1983), *vol.* 126, *pp.* 521–532
Printed in Great Britain

Oscillatory Hele-Shaw convection

By H. FRICK
Institute of Geophysics and Planetary Physics, University of California, Los Angeles

AND U. MÜLLER
Kernforschungszentrum Karlsruhe, Institut für Reaktorbauelemente, Karlsruhe, West Germany

Received 25 February 1982 and in revised form 1 July 1982)

Time-dependent convection motions in the form of rolls in a thin vertical fluid layer (Hele-Shaw cell) heated from below are investigated numerically. Perpendicular to the convection-roll axis the fluid is bounded by parallel adiabatic rigid sidewalls. Stress-free top, bottom and end boundaries are assumed. The horizontal extension of the convection rolls is described by the wavenumber α. Solutions for the time-dependent behaviour of the convective motion are presented for a range of wavenumbers between $\alpha = \frac{1}{2}\pi$ and 2π. The onset of the oscillation is shifted to higher Rayleigh numbers with increasing wavenumber. The oscillatory Hele-Shaw convection is caused by an instability of the thermal boundary layer, as is evident from the plotted temperature field and streamlines. From the variation of the Nusselt number with time it is found that the oscillatory motion starts with a sinusoidal time dependence and passes into a periodic state with several frequencies as the Rayleigh number is increased. Quantitative and qualitative agreement with previous experimental and numerical results is found.

1. Introduction

In recent years investigations of convection in a fluid layer of infinite horizontal extent heated from below have led to a good understanding of the flow pattern. This system is one of the simplest hydrodynamical examples in which the transition to turbulence from a simple state can be studied (Clever & Busse 1974; Busse 1978). The evolution of turbulence occurs over several discrete transitions. Among these the transition to oscillatory convection represents an important state in the understanding of the development of turbulence. A summarizing diagram of the visually observed transitions in convection as a function of Rayleigh and Prandtl numbers is given by Krishnamurti (1970*a*, *b*; 1973) and a slightly modified version presented by Busse (1978). Depending on the Prandtl number, two-dimensional convection changes into various forms of three-dimensional steady and unsteady forms of convection with increasing Rayleigh number. In recent experiments on unsteady thermal convection in layers where the height becomes comparable with the width (aspect ratio $A = 1$), the use of laser-Doppler velocimetry or thermocouples for temperature measurements (Ahlers & Behringer 1978; Berge & Dubois 1979; Maurer & Libchaber 1979; Gollub & Benson 1980) has made it possible to obtain measurements of convection flow. By the use of Fourier spectra of the signals it was found that the transition from the steady to the chaotic time-dependent state starts with the onset of periodic

oscillations, followed by a quasiperiodic oscillation with 2 or 3 incommensurate frequencies and the possibility of phase locking.

Another excellent example for studying the transition to turbulence theoretically as well as experimentally is the behaviour of the convection flow in a thin vertical layer with adiabatic sidewalls, the so-called Hele-Shaw cell. The peculiarity of the Hele-Shaw flow as opposed to the classical Rayleigh–Bénard problem is that the flow is always two-dimensional and independent of the Prandtl number. Free convection in Hele-Shaw cells has also been used to simulate thermal convection in porous media (Wooding 1960; Elder 1967; Horne & O'Sullivan 1974; Hartline & Lister 1977; Kvernvold 1979). The analogy between slow two-dimensional flow in a porous medium and laminar flow in a narrow slot with two parallel walls was first shown by Hele-Shaw (1898). The analogy is made obvious by defining an appropriate permeability, as Hartline & Lister (1977) have done. Kvernvold (1979) has used the governing equations for motion in a Hele-Shaw cell following Hartline & Lister (1977) in order to investigate the stability of the stationary solutions with respect to infinitesimal disturbances. His results show that the Hele-Shaw convection is stable for a much wider range of wavenumbers and Rayleigh numbers than ordinary porous-media convection. The geometry of the Hele-Shaw cell forces the disturbances to be purely two-dimensional, and thus only the Eckhaus and the oscillatory instabilities can exist. The onset of oscillatory convection is dependent on wavenumber α and Rayleigh number R. The stable motion is limited by the oscillatory instability from $\alpha > 0{\cdot}4\alpha_c$ and $R = 3{\cdot}8R_c$ up to $\alpha = \alpha_c = \pi$ and $R = 8R_c$ (Kvernvold 1979 and private communication 1980). The experimental investigation of Koster (1980) shows the onset of time-dependent convection at $R/R_c = 10{\cdot}3$ for $\alpha/\alpha_c = 1$. The theoretical results of Caltagirone (1975) for the comparable two-dimensional flow in porous media show that unicellular convection becomes unsteady for Rayleigh numbers exceeding $R/R_c = 10$, while Schubert & Straus (1979) report about a value of $R/R_c = 8$. In the case of porous media the critical Rayleigh number R_c is known to be $R_c = 4\pi^2$ (Horton & Rogers 1945; Lapwood 1948). For a Hele-Shaw cell, considered as a thin vertical channel with an aspect ratio $A \gg 20$ ($A = h/d$, the ratio of channel height to channel width), Frick & Clever (1980) have determined the critical value $R_c = (4\pi^2)\,12A^2$. The analysis of time-dependent Hele-Shaw convection (Koster 1980) shows that the transition from the steady to the chaotic state is preceded by the onset of periodic and then quasiperiodic oscillations, similar to the behaviour of convection in a thin horizontal fluid layer.

The main goal of the present paper is to study the time-dependent behaviour of the Hele-Shaw convection and to determine the relationship between the Nusselt number, the isotherms and the streamlines for several Rayleigh numbers. Since the mathematical analysis of steady convection rolls has been described in an earlier paper (Frick & Clever 1982), only a brief discussion of the numerical techniques is given in §2. The numerical results are presented and discussed in §3. Some concluding remarks are made in §4.

2. Mathematical formulation of the problem

We consider a long vertical fluid layer heated from below of height h and with parallel sidewalls a distance d ($d \ll h$) apart. The horizontal boundaries are free. Constant temperatures T_1 and T_0 are prescribed at the upper and lower boundaries of the layer, where T_0 is larger than T_1. The lateral walls are insulated. The size of the convection rolls is given by the wavenumber α. The theoretical description of

problem is based on the Navier–Stokes equations and the heat equation in the Boussinesq approximation. A complete mathematical description of the problem is given in Frick & Clever (1982).

In the limit of Hele-Shaw convection ($d \ll h$) it is possible to use a simplified representation for the velocity field

$$\mathbf{v} = \boldsymbol{\varepsilon}\psi = \nabla \times (\mathbf{j}\psi), \tag{1}$$

where $\mathbf{j}$ is the unit vector in the direction of the channel width d. By introducing dimensionless quantities, after operating with $\boldsymbol{\varepsilon}$ on the equation of motion, we obtain the following equations in the limit of infinite Prandtl number for ψ and θ:

$$\nabla^2 \Delta_2 \psi + \partial_x \theta = 0, \tag{2}$$

$$\nabla^2 \theta + R\,\partial_x \psi = -\partial_z \psi\, \partial_x \theta + \partial_x \psi\, \partial_z \theta + \partial_t \theta, \tag{3}$$

where θ is the deviation from the temperature distribution of the static state. The Laplacians Δ_2 and ∇^2 are defined by

$$\Delta_2 = \partial_{xx}^2 + \partial_{zz}^2, \tag{4}$$

$$\nabla^2 = \partial_{xx}^2 + A^2\,\partial_{yy}^2 + \partial_{zz}^2. \tag{5}$$

The dependence of the problem on the physical conditions of the fluid layer has been reduced to the Rayleigh number R and the aspect ratio A:

$$R = \frac{\gamma g \Delta T h^3}{\nu \kappa}, \quad A = \frac{h}{d}, \tag{6}$$

where γ is the coefficient of thermal expansion, g is the acceleration due to gravity, $\Delta T = T_0 - T_1$ is the temperature difference, ν is the kinematic viscosity and κ is the thermal diffusivity.

As in the previous investigation (Frick & Clever 1982) we use the Galerkin technique to solve (2) and (3), where ψ and θ are expanded in terms of orthogonal functions. The various trial functions for ψ and θ are given by Frick & Clever (1982). In the case of Hele-Shaw convection caused by the parabolic flow and uniform temperature profile across the channel width (Frick 1981) it is possible to reduce the number of functions in the y-direction, when the aspect ratio A is large. In the present study we use an aspect ratio $A = 1000$. An acceptable solution has been obtained when the Nusselt number changes by less than 1·5 % as the truncation parameter N is increased to $N+2$. The values of the truncation parameter chosen depend on the Rayleigh number and wavenumber, and are comparable with those given by Schubert & Straus (1979).

3. Discussion of results

In describing the numerical results for unsteady convection rolls we shall explain the time-dependent behaviour of the convective heat transport, isotherms and streamlines. For three examples of wavenumbers, $\alpha = \frac{1}{2}\pi$ (large convection rolls), $\alpha = \alpha_c = \pi$ (rolls with a height equal to the length), and $\alpha = 2\pi$ (small rolls), the problem of the oscillatory convection is discussed in terms of the ratio R/R_c of the actual to the critical Rayleigh number.

In discussing the time-dependent behaviour of the Hele-Shaw convection for several wavenumbers we first consider rolls with $\alpha = \frac{1}{2}\pi$. For this wavenumber the convection is steady up to a Rayleigh number $R/R_c = 6$. With increasing R the flow

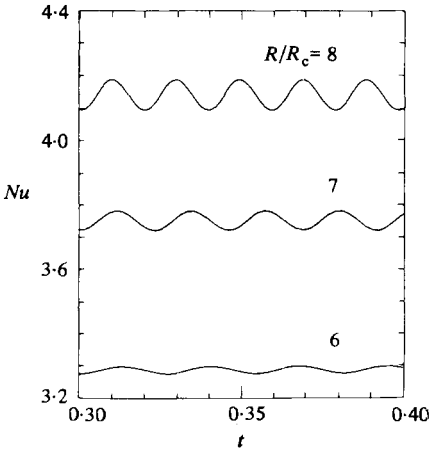

FIGURE 1. Nusselt-number variations with time t at several values of R/R_c for $\alpha = \frac{1}{2}\pi$.

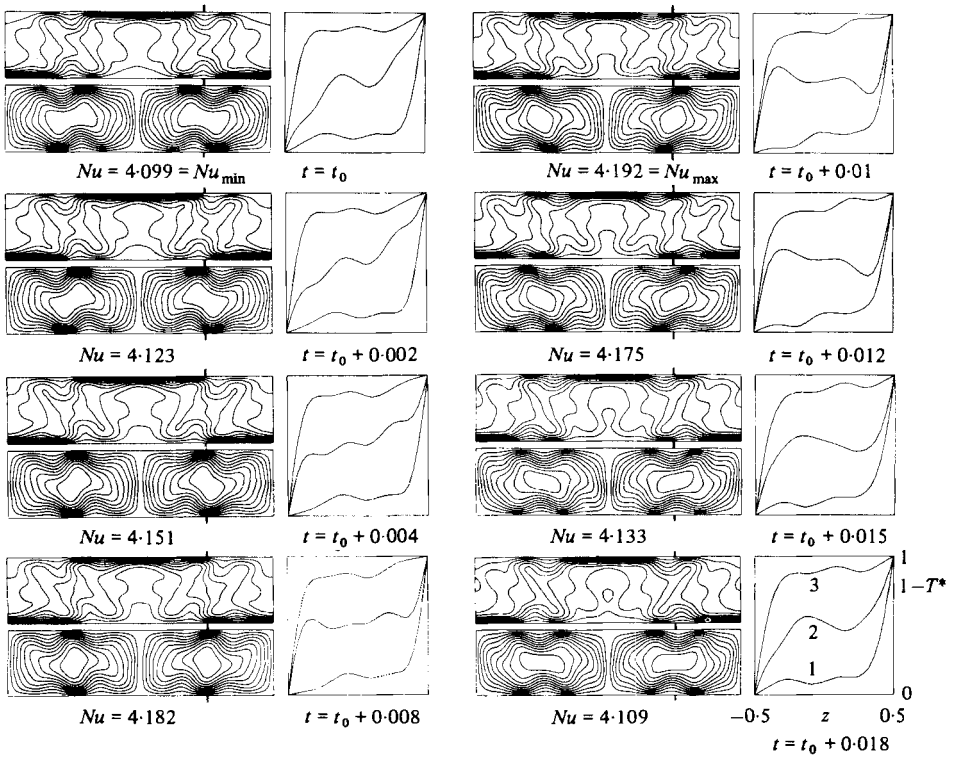

FIGURE 2. Time dependence of the isotherms and streamlines at $R/R_c = 8$ for $\alpha = \frac{1}{2}\pi$.

shows an oscillatory behaviour and the heat transport becomes time-dependent. Figure 1 illustrates how the Nusselt-number fluctuations with time change for several Rayleigh numbers. The motion is typically time-periodic with a period τ. With increasing R/R_c the period τ decreases, while the amplitudes of the Nu-fluctuations become larger. The main source of unsteady flow can be seen in figure 2 in which a

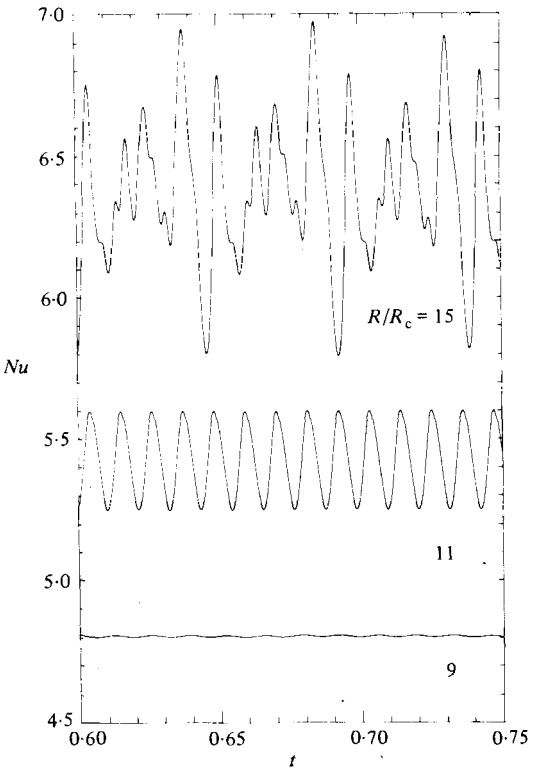

FIGURE 3. Nusselt number as a function of time at several Rayleigh numbers for $\alpha = \pi$.

time series of isotherms and streamlines is shown at the vertical centreplane of the channel. Wavy perturbations occur in the temperature boundary layer in a region of maximized temperature gradient, for example near the lower boundary close to the position of the downward convection, and move towards the zone of upward flow. This process can be explained as an instability of the boundary layer at the lower and upper sides. Because the local temperature gradient exceeds a critical value, small secondary convection eddies develop in this layer. The movement of the wavy perturbations results from a superposition of the basic convection roll with these secondary eddies. These perturbations decrease the heat transport locally and this effect intensifies with increasing Rayleigh number. The time dependence of the temperature distribution T^* versus the height of the fluid layer (z-direction) in the centre (1) and in the zones of upflow (3) and downflow (2) of the convection cells demonstrates these local modifications in figure 2. As seen in figure 2 parcels of hot fluid are advected along the lower boundary towards the region of ascending motion. In the second row of pictures the two parcels arriving at centre from both sides combine and form a hot blob separating from the boundary. At the same time the Nusselt number based on the average temperature gradient at the boundary decreases. An equivalent process is to observe at the upper side. Owing to the relatively large convection rolls ($\alpha = \frac{1}{2}\pi$) it is possible to have two wavy perturbations in the region of one convection roll. This is clearly seen in the contour plots of the isotherms and streamlines for $Nu_{\max}$ in figure 2. In the case $\alpha = \frac{1}{2}\pi$ the wavy perturbations need a time of 2 periods τ to evolve and to disappear.

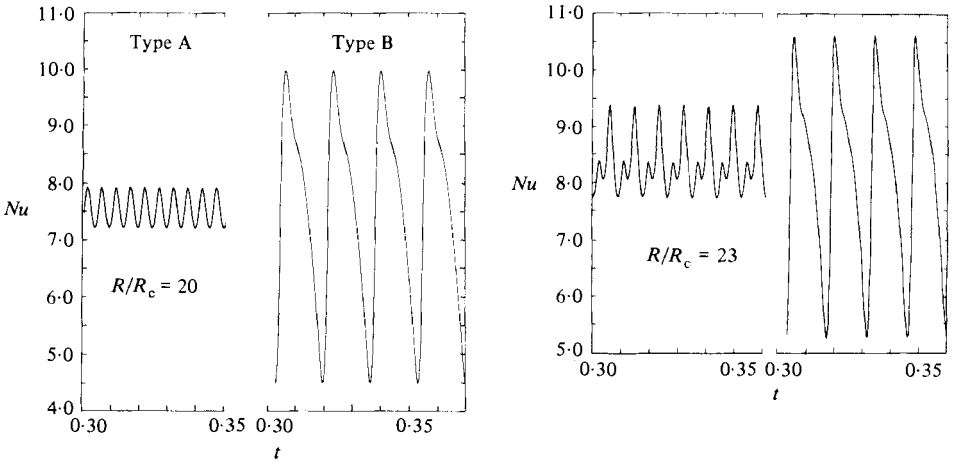

FIGURE 4. Nusselt-number fluctuations with time at $R/R_c = 20$ and $R/R_c = 23$ for $\alpha = 2\pi$.

With increasing wavenumber the onset of the oscillation is shifted to higher values of R/R_c. For $\alpha = \pi$ the time-dependent convection begins at $R/R_c > 9$ and shows a periodic behaviour with a single frequency up to $R/R_c = 11$ (figure 3). As in the case of $\alpha = \frac{1}{2}\pi$ the period τ decreases, while the amplitudes of the Nusselt fluctuations become larger. The unsteady behaviour is attributed to a movement of one wavy perturbation along the horizontal sides, as shown theoretically by Caltagirone (1975) and experimentally by Koster (1980). At $R/R_c = 15$ the motion becomes periodic with several frequencies. The Nusselt-number fluctuations show a number of different large maxima and minima, which are periodic in time of order τ_1. Two maxima are remarkable, $Nu = 6{\cdot}95$ and $Nu = 6{\cdot}8$, a time τ_2 apart, where τ_2 is a rational fraction of τ_1.

A new kind of unsteady behaviour is found in the case of small convection rolls with a wavenumber $\alpha = 2\pi$. In the range of Rayleigh numbers investigated, $18 \leqslant R/R_c \leqslant 23$, two types of fluid motion have been found. The first type has a similar flow character to the case $\alpha \leqslant \pi$; we shall refer to this as type A. The other type of flow (type B) consists of oscillatory motion that is symmetric with respect to the original centre of the roll. This motion can be described as an oscillation of a diagonal roll with two secondary rolls in the opposite corners. Figure 4 illustrates how the Nu-fluctuations change with time from $R/R_c = 20$ up to $R/R_c = 23$ for both types of motion. The time dependence of Nu is plotted for type A in the left part of each diagram and for type B in the right part. First we shall discuss the time dependence of type-A convection.

At the onset of convection ($R/R_c > 18$) the motion is typically time-dependent with a single frequency, and with increasing Rayleigh number ($R/R_c = 23$) the Nu-fluctuations show a transition to a periodic behaviour with several frequencies. A characteristic property of this form of convection (at $R/R_c = 20$) is the rise of one small blob of hot fluid from the lower hot layer into the colder region before the minimum of the Nusselt number is reached. The time-dependent behaviour of the convection motion at $R/R_c = 23$ can be observed in figure 5, in which a time series of isotherms and streamlines is shown. It is remarkable that two fluid blobs emerge from the boundary layer even though the basic wavelength of the rolls is relatively small. In figure 5 wavy perturbations of two different strengths (indicated by I and

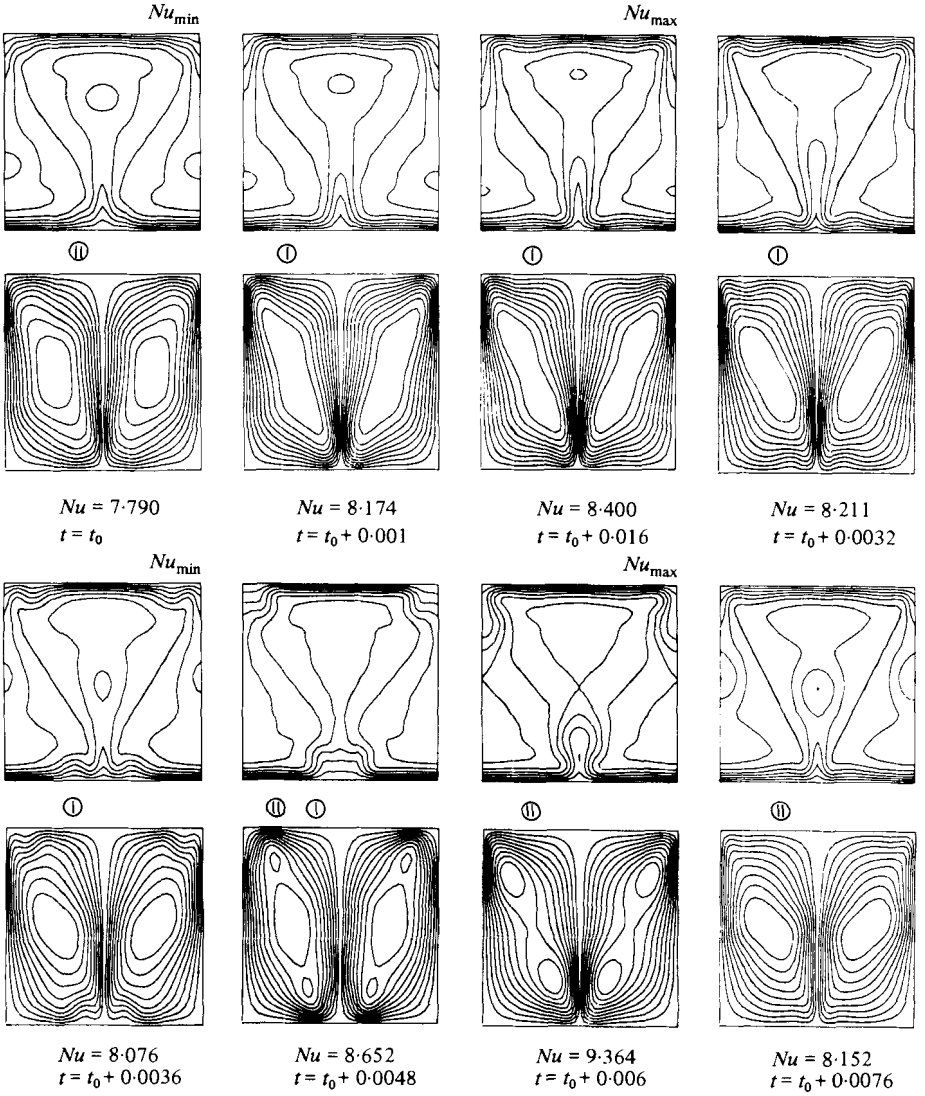

FIGURE 5. Isotherms and streamlines pattern of type-A flow at $R/R_c = 23$ and $\alpha = 2\pi$.

II) give rise to warm fluid blobs of different size. The oscillatory peaks in the Nusselt number in figure 4 correspond to this process.

The other fundamental time-dependent behaviour is that of type B. A characteristic feature of this flow is the existence of large fluctuations of the Nusselt number (figure 4) with varying slopes. In figure 6 the patterns of the isotherms and streamlines are shown in connection with the fluctuations in time of the Nusselt number at $R/R_c = 23$. The minimum of the heat transport (1) develops when a large diagonal roll exists with two very small rolls in the opposite corners. As time goes on, the corner cells increase, and the basic roll is squeezed in the middle. At the same time the Nusselt number increases. The maximum of Nusselt number is reached when the diagonal and the corner roll have about the same width near the horizontal boundaries (2). With increasing corner-roll size the basic roll is divided into two parts and results in four cells (4). Then the original rolls begin to increase in size and form

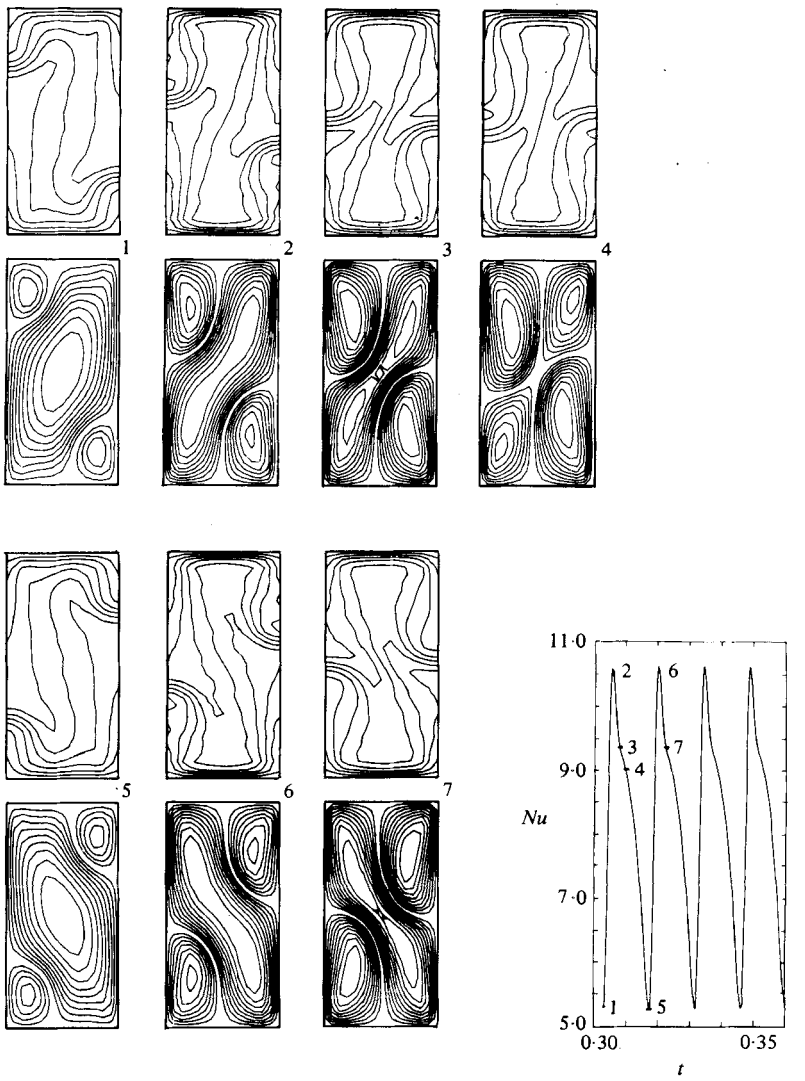

FIGURE 6. Time variation of isotherms and streamlines in comparison with the Nusselt-number fluctuations of type-B flow at $R/R_c = 23$ and $\alpha = 2\pi$.

a new roll in the opposite diagonal (5). This process forces a decrease in the Nusselt number until a new squeezing of the diagonal roll occurs (5) and the same time-dependent process repeats itself. The original position of the diagonal roll (1) is thus found again after a time of two periods of the Nusselt-number variation.

After having considered the characteristic behaviour of flows of both type A and B, we shall now discuss the calculated solutions in relation to the types of flow that have been observed experimentally. The numerical investigations have shown that both types of solution may develop for the same value of R. Whether type-A or type-B solutions are obtained depends on the numerical procedure used. Upon increasing the Rayleigh number above the steady state for $R/R_c = 17$ and $\alpha = 2\pi$, oscillatory solutions of type A have been found when a truncation parameter large enough to obtain converged solutions was used. The optical investigations of Koster (1980) for

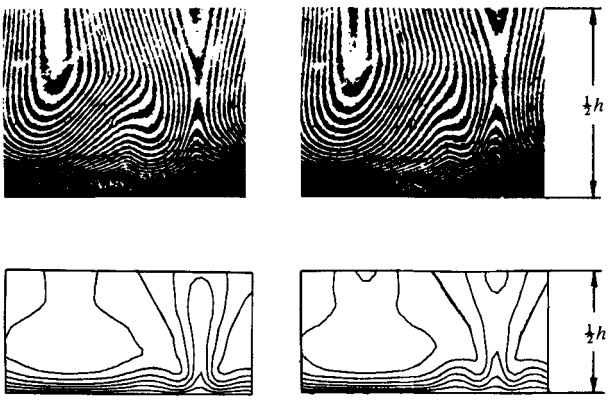

FIGURE 7. Comparison of temperature-field sections with experimental measurements by Koster (1980), demonstrating instability of the boundary layer at the bottom of a Hele-Shaw cell. (Experiment: $\alpha = 8{\cdot}3$, theory: $\alpha = 2\pi$.)

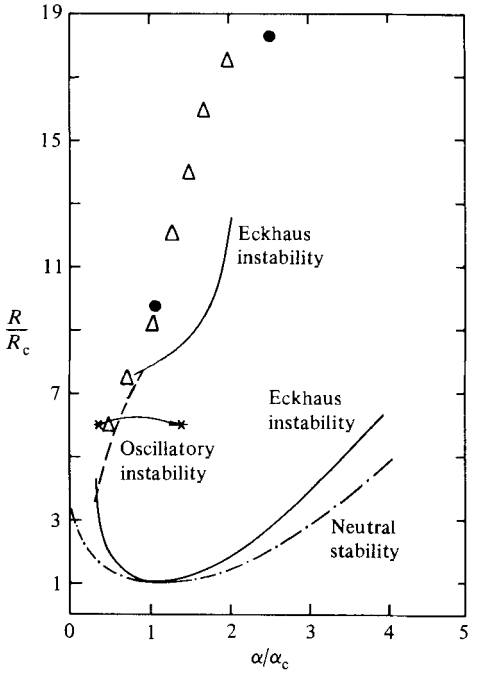

FIGURE 8. Stability diagram of Hele-Shaw convection rolls.

the time-dependent behaviour of Hele-Shaw convection also show this flow type for large wavenumbers. Experimental and theoretical characteristic temperature fields of type-A flow are shown in figure 7. From these sections the movement of the previously discussed wavy perturbations is easy to recognize in the boundary layer.

Time-dependent flow behaviour of type B, consisting of an oscillatory motion of a diagonal roll and two secondary rolls, has been found for calculations starting with a strongly reduced truncation parameter. When this unconverged solution was used as the initial solution for calculations with high truncation parameter, the result was a numerically converged solution of type B. Thus converged solutions of both types

A and B can be generated depending on the initial conditions. When the Rayleigh number is increased in steps of $\Delta(R/R_c) = 1$ while employing a high truncation parameter, the solution of type B continues to be obtained. Large jumps in the Rayleigh number (about $\Delta(R/R_c) = 3$) cause a change in the time-dependent behaviour and lead to a solution of type A. Thus flow of type B tends to be unstable to sufficiently large disturbances. Oscillatory convection of type B has been experimentally observed (Putin & Tkacheva 1979; Koster 1980) in Hele-Shaw finite boxes of small aspect ratio A^* for $A^* = 2$ and $A^* = 3{\cdot}5$ (A^* = height/length).

A question of fundamental interest is the stability of the steady flow. The theoretical investigation of the stability of the two-dimensional Hele-Shaw convection has been made by Kvernvold (1979 and private communication 1980). His results are given in figure 8. The different states are distinguished by the ratios R/R_c and α/α_c. The boundaries for onset of convection and for Eckhaus and oscillatory instabilities are marked by dash-dotted, solid, and dashed lines respectively. Also shown in figure 8 are the results for the onset of time-dependent convection (circles are for the experimental work of Koster (1980); triangles indicate the numerical results of this paper). Beside the cases $\alpha = \frac{1}{2}\pi$, $\alpha = \pi$ and $\alpha = 2\pi$, already discussed, additional wavenumbers have been investigated so that the boundary of the oscillatory instability can be more accurately determined. Time-dependent calculations for smaller values, such as $\alpha = \frac{1}{2}\pi$ and $R/R_c = 6$, do not yield oscillatory solutions because the initially large-wavelength rolls disintegrate into smaller rolls, as indicated by asterisks and the arrow in figure 8.

4. Conclusion

The Galerkin method has been applied to the problem of time-dependent convective motion in a Hele-Shaw cell. The numerical results agree both quantitatively and qualitatively with the results of the experiments of Koster (1980). The oscillatory convection is dependent on the Rayleigh number and the wavenumber. The Rayleigh number for the onset of oscillations increases to higher values with increasing wavenumber.

The phenomena of oscillatory Hele-Shaw convection have been attributed to an instability of the thermal boundary layer as shown by the isotherm pattern (Koster 1980). A similar conclusion is reached by theoretical considerations following Howard (1964) and Busse (1978). The transition from steady to unsteady convection in a Hele-Shaw cell is comparable to the onset of bimodal convection for the Bénard case (a thin horizontal fluid layer) for infinite Prandtl number. The origin of the transition to bimodal convection also lies in the instability of the thermal boundary layer (Busse 1978). But in the Bénard case secondary rolls develop perpendicular to the main roll in the boundary layer and the result is a three-dimensional motion. In contrast with this, the time-dependent Hele-Shaw convection is caused by the advection of the secondary eddies by the basic roll motion.

The pattern of oscillatory Hele-Shaw convection has been visualized by the time dependence of isotherms, streamlines and heat transport. In agreement with the experimental evidence, the time-dependent motion starts as a sinusoidal oscillation and passes into a periodic state with several frequencies as the Rayleigh number increases. At the same time, the period decreases, while the amplitudes of the Nusselt-number fluctuations increase. The computational results presented here complement the optical investigation of Koster (1980) and the numerical studies of

Caltagirone (1975) and Schubert & Straus (1979). The oscillatory stability boundary in the Hele-Shaw stability diagram given by Kvernvold (1979 and private communication 1980) has been confirmed for wavenumbers $\alpha = \frac{1}{2}\pi$ and extended up to $\alpha = 2\pi$. Although a transition to quasiperiodic and aperiodic behaviour is likely to occur at higher Rayleigh numbers, computational expenses have so far prevented us from investigating those regions.

The authors wish to thank Prof. F. H. Busse and Dr R. M. Clever for many helpful discussions and for their assistance in preparing the manuscript. This work was supported by the Deutsche Forschungsgemeinschaft.

REFERENCES

AHLERS, G. & BEHRINGER, R. P. 1978 Evolution of turbulence from the Rayleigh–Bénard instability. *Phys. Rev. Lett.* **40**, 711.

BERGE, P. & DUBOIS, M. 1979 Study of unsteady convection through simultaneous velocity and interferometric measurements. *J. Phys. Lett.* **40**, 505.

BUSSE, F. H. 1978 Non-linear properties of thermal convection. *Rep. Prog. Phys.* **41**, 1929.

CALTAGIRONE, J. P. 1975 Thermoconvective instabilities in a horizontal porous layer. *J. Fluid Mech.* **72**, 269.

CLEVER, R. M. & BUSSE, F. H. 1974 Transition to time-dependent convection. *J. Fluid Mech.* **65**, 625.

ELDER, J. W. 1967 Steady free convection in a porous medium heated from below. *J. Fluid Mech.* **72**, 29.

FRICK, H. 1981 Zellularkonvektion in Fluidschichten mit zwei festen seitlichen Berandungen. Dissertation, Universität Karlsruhe (KfK 3109).

FRICK, H. & CLEVER, R. M. 1980 Einfluss der Seitenwände auf das Einsetzen der Konvektion in einer horizontalen Flüssigkeitsschicht. *Z. angew. Math. Phys.* **31**, 502.

FRICK, H. & CLEVER, R. M. 1982 The influence of side walls on finite-amplitude convection in a layer heated from below. *J. Fluid Mech.* **114**, 467.

GOLLUB, P. & BENSON, S. V. 1980 Many routes to turbulent convection. *J. Fluid Mech.* **100**, 449.

HARTLINE, B. K. & LISTER, C. R. B. 1977 Thermal convection in a Hele-Shaw cell. *J. Fluid Mech.* **79**, 379.

HELE-SHAW, H. S. J. 1898 Investigations of the nature of surface resistance of water and a stream motion under certain experimental conditions. *Trans. Inst. Nav. Arch.* **40**, 21.

HORNE, R. N. & O'SULLIVAN, M. J. 1974 Oscillatory convection in a porous medium heated from below. *J. Fluid Mech.* **66**, 339.

HORTON, C. W. & ROGERS, F. T. 1945 Convection currents in a porous medium. *J. Appl. Phys.* **16**, 367.

HOWARD, L. N. 1964 Convection at high Rayleigh number. In *Proc. 11th Int. Congr. on Appl. Mech., Munich* (ed. H. Görtler), p. 1109. Springer.

KOSTER, J. N. 1980 Freie Konvektion in vertikalen Spalten. Dissertation, Universität Karlsruhe (KfK 3066).

KRISHNAMURTI, R. 1970*a* On the transition to turbulent convection. Part 1. The transition from two- to three-dimensional flow. *J. Fluid Mech.* **42**, 295.

KRISHNAMURTI, R. 1970*b* On the transition to turbulent convection. Part 2. The transition to time-dependent flow. *J. Fluid Mech.* **42**, 309.

KRISHNAMURTI, R. 1973 Some further studies on transition to turbulent convection. *J. Fluid Mech.* **60**, 285.

KVERNVOLD, O. 1979 On the stability of non-linear convection in a Hele-Shaw cell. *Int. J. Heat Mass Transfer* **22**, 395.

LAPWOOD, E. R. 1948 Convection of a fluid in a porous medium. *Proc. Camb. Phil. Soc.* **44**, 508.

MAURER, J. & LIBCHABER, A. 1979 Rayleigh–Bénard experiment in liquid helium: frequency locking and onset of turbulence. *J. Phys.* (*Paris*) **40**, 419.

PUTIN G. F. & TKACHEVA, E. A. 1979 Experimental investigation of supercritical convective motions in a Hele-Shaw cell. *Izv. Akad. Nauk SSSR, Mekh. Zhid. i Gaza* **14**.

SCHUBERT, G. & STRAUS, J. M. 1979 Three-dimensional and multicellular steady and unsteady convection in fluid-saturated porous media at high Rayleigh numbers. *J. Fluid Mech.* **94**, 25.

WOODING, R. A. 1960 Instability of a viscous liquid of variable density in a vertical Hele-Shaw cell. *J. Fluid Mech.* **7**, 501.